Journal of Photochemistry and Photobiology A: Chemistry 212 (2010) 101–106

Contents lists available at ScienceDirect

Journal of Photochemistry and Photobiology A: Chemistry

journal homepage: www.elsevier.com/locate/jphotochem

Photocatalytic decolourization of indigo carmine on 1,10-phenanthrolinium intercalated bentonite under UV-B and solar irradiation

Abdelhadi Bentouami[a,b,*], Mohand Said. Ouali[b], Louis-Charles De Menorval[c]

[a] Université des Sciences et Technologie d'Oran « M. Boudiaf », Faculté des Sciences, Département de Chimie, BP 1505, Oran El M'Nouer, Algeria
[b] Laboratoire de Valorisation des Matériaux, University of Mostaganem, BP 466, Mostaganem R.P., Algeria
[c] ICG–AIME–UMR 5253, Université Montpellier 2, Place Eugène Bataillon CC 1502, 34095 Montpellier Cedex 05, France

ARTICLE INFO

Article history:
Received 19 November 2009
Received in revised form 25 March 2010
Accepted 2 April 2010
Available online 8 April 2010

Keywords:
Bentonite
Solar irradiation
Photo-decolourization
Indigo carmine

ABSTRACT

In the present work, organophilic clay was prepared and characterized by XRD, FT-IR, TGA, ^{13}C MAS NMR and UV–vis DRS. The obtained material was investigated as photocatalyst on photo-decolourization of indigo carmine under UV-B and solar irradiation. The decolourization capacity of the obtained material against indigo carmine was very low. Besides, the kinetic photo-decolourization data under UV-B and solar irradiation fitted well the pseudo-first order and Langmuir–Hinshelwood kinetic models. The photo-decolourization rate was found better under solar than UV-B irradiation. A total colour removal was obtained at natural pH after 160 min of solar irradiation of a 10 mg L^{-1} indigo carmine solution. The prepared material was used four times with practically the same decolourization efficiency.

1. Introduction

Indigo carmine (IC), a blue synthetic dye, is used in textile industry for dyeing of clothes (blue jeans) and other blue denims, in cosmetics industries, in medicine as a diagnostic aid (e.g. in kidney function tests [1]) and it has also been employed as redox indicator in analytical chemistry and as a microscopic stain in biology [2]. IC is also used as a photometric detector. However, IC dye causes irritation to the gastrointestinal tract leading to nausea, vomiting and diarrhea [3]. It may also cause irritation to the respiratory tract. Symptoms may include coughing and shortness of breath [4]. IC containing effluents are generated from textiles, printing and dyeing, paper, cosmetics, plastics industries, etc. [5].

The removal of dyes from industrial effluents poses a major problem although conventional treatment processes such as coagulation–flocculation [6–8], adsorption [9–11], membrane filtration [12] and chemical oxidation [13–15] and so on are available. Most of these processes are however costly and particularly ineffective when treating wastewaters containing low concentrations of dyes.

During the last decade, more attention has been focused on the development of new treatment technologies that lead to complete decomposition of dye molecules [16–20]. Among these treatments, advanced oxidation processes (AOPs) represent a powerful alternative to conventional treatment methods for wastewater decontamination [21]. In heterogeneous photocatalysis, it has been shown the efficiency of semiconductor oxides like TiO_2, ZnO and CdS [22] on decolourization of and mineralization of several dyes using either UV or solar light [23–27].

Clay-based materials, principally pillared clays (PILCs) have recently been used as solid supports for the encapsulation of transition metal complexes. This approach offers an alternative route for the conception of heterogeneous catalysts having metal–complex–clay hybrid structure [28–30]. The deposition of metal complex into the clay is usually achieved by ion exchange and dry impregnation techniques. Francisco and co-workers [31] also reported the encapsulation of metal complex into the large pores of Al-PILC. Most of these metal complex–clay hybrids were tested in a variety of catalytic oxidation processes in the dark [29,32,33].

So far however, research on heterogeneous photocatalytic decolourization of dyes by modified clays still scarce, though when going through the few published papers dealing with this topic, we found that oxidative reagents such as H_2O_2 are always employed in order to promote the degradation process. In this context, Sanabria et al. [34] reported the use of pillared bentonite with solid Al–Fe polyhydroxycation in the catalytic oxidation of phenol with H_2O_2. Cheng et al. [35] also tested the catalytic activity of iron species in layered clays for the photo-degradation of organic dyes under visi-

* Corresponding author at: Université des Sciences et Technologie d'Oran « M. Boudiaf », Faculté des Sciences, Département de Chimie, BP 1505, Oran El M'Nouer, Algeria. Tel.: +213 771 90 61 44; fax: +213 41 56 03 62.
E-mail addresses: a-bentouami@univ-usto.dz, bentouami@gmail.com (A. Bentouami), ouali@univ-mosta.dz (M.Said. Ouali), lcdemenorval@univ-montp2.fr (L.-C. De Menorval).

1010-6030/$ – see front matter © 2010 Elsevier B.V. All rights reserved.
doi:10.1016/j.jphotochem.2010.04.002

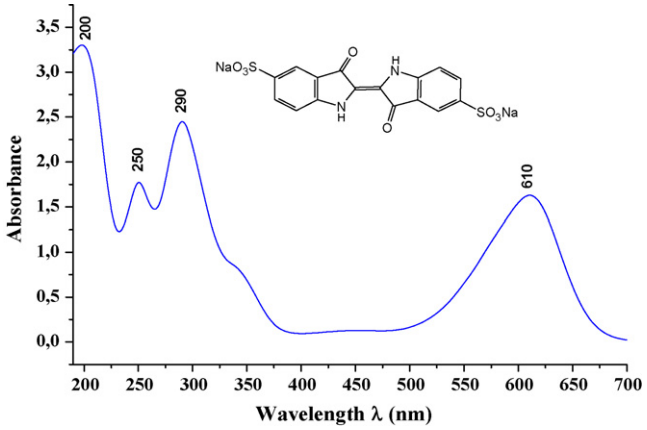

Fig. 1. Structure and UV–vis spectrum of indigo carmine dye (10^{-4} M).

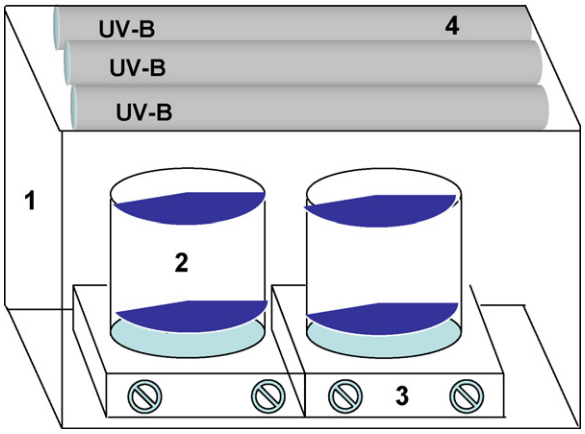

Fig. 2. Experimental photo-decolourization set up (1: aquarium mirror, 2: open Pyrex cells of 500 mL capacity, 3: magnetic stirrers, 4: UV lamps).

ble irradiation using H_2O_2 as oxidant, while Feng et al. [36] reported the use of a bentonite-based Fe nanocomposite film as a heterogeneous photo-Fenton catalyst for the decolourization of orange II. Cheng et al. [37] synthesized a metal–complex–clay material using laponite clay as host and iron(II) 2,2′-bipyridine complex as guest, the obtained material has tested as a catalyst in the photodegradation of organic pollutants in the presence of H_2O_2 under visible irradiation. As shown in these previous works, H_2O_2 is involved with the catalyst (metal–complex–clay) in the decolourization and degradation of pollutants and where UV, visible or solar irradiations might accelerate the oxidation reactions.

As far as we know, reports claiming the use of intercalated bentonite with organic compounds in photo-decolourization processes are lacking in the literature. In this paper, we report the first example of ion organic intercalated bentonite material never investigated in the photocatalytic decolourization of dyes. The material has been synthesized by inserting 1,10-phenanthrolinium cation into bentonite interlayer space, and was employed as catalyst support in the photo-degradation of indigo carmine (anionic dye) under UV-B and solar irradiations without resorting to the use of any oxidant.

2. Experimental

2.1. Starting materials

Raw bentonite originated from Maghnia deposit (West of Algeria), was purified as described in our previous work [38] by sedimentation, the <2 μm fraction was exchanged three times with molar NaCl solution and washed with distilled water until excess Cl^- ions were not detectable by $AgNO_3$ test. Previous studies indicate that the main component of this bentonite is montmorillonite [39]. Its cation exchange capacity (CEC), measured according to Kahr and Madsen [40], was 0.91 mol/kg. Chemical composition of the sodic bentonite (B-Na) is given in Table 1 [41].

Indigo carmine (IC) (anionic dye) [3,3′-dioxo-1,3,1′,3′-tetrahydro-[2,2′]-bi-indolylidene-5,5′-disulfonic acid disodium salt] MF $C_{16}H_8N_2Na_2O_8S_2$, MW = 466.35 g/mol, was analytic grade. The molecular structure and the UV–vis absorption spectrum of indigo carmine are presented in Fig. 1.

2.2. Preparation of orthophenanthrolinium exchanged bentonite

10 g of sodic bentonite (B-Na) was suspended in a 15 mmol L^{-1} solution of monochlorhydrate orthophenanthrolinium ($C_{12}H_8N_2{\cdot}HCl{\cdot}H_2O$) (oPhen) and the mixture was stirred at room temperature for 48 h. The solid phase (B-oPhen) was separated by centrifugation and was then washed with distilled water until excess orthophenanthrolinium ions were not detected by ferrous test (red colour). The solid was dried in the oven at 80 °C, crushed and 50 μm sieved.

X-ray powder diffraction data were collected with monochromatic Cu Kα radiation (λ = 1.540589 Å) using a PHILIPS X'Pert MPD diffractometer. FT-IR spectra of B-Na and B-oPhen (KBr disc samples) were recorded on a NICOLET Avatar 330 FT-IR spectrophotometer in the region of 400–4000 cm^{-1}. Thermogravimetric analyses (TGA) were performed with a Netzsch TGA 409 PC thermo balance with a heating rate of 20 °C min^{-1} from 25 to 900 °C. The diffuse reflectance spectra of the B-oPhen and B-Na were recorded on a UV–vis spectrophotometer (Perkin Elmer Lambda 14) equipped with an integration sphere.

2.3. Determination of intercalated orthophenanthrolinium amount

To 50 mg of B-oPhen was added 100 mL of 0.01 M $NaNO_3$ aqueous solution and the suspension was stirred at room temperature for 1 h and then centrifuged. The supernatant was analyzed in presence of Fe^{2+} ions by UV–vis at 510 nm using a HACH DR/4000U spectrophotometer. The calibration curve was established on orthophenanthrolinium solutions using the same conditions. The exchangeable amount of orthophenanthrolinium per gram of bentonite was determined to be 0.185 mmol/g which corresponds to 20.3% of the total CEC.

2.4. Apparatus

Photo-decolourization investigations were performed in a 500 mL open Pyrex cell placed in an aquarium box walled up with inner mirrors (Fig. 2) and equipped with 3 parallel UV-B lamps (8 W

Table 1
Chemical composition of sodic bentonite.

	Oxide							
	SiO_2	Al_2O_3	CaO	MgO	Fe_2O_3	Na_2O	K_2O	SiO_2/Al_2O_3
%	59.40	23.13	0.59	2.60	2.49	3.17	0.88	2.57

at 315 nm). Under solar irradiation, the experiments were carried in sunny and clear days during April between 10 am and 4 pm in our laboratory of Mostaganem (latitude: 35°54′N, longitude: 0°4′E). A 500 mL open Pyrex cell placed on a flat surface was used.

2.5. Procedure

All experiments were carried out by stirring suspensions of B-oPhen or B-Na (0.25 g) in 250 mL of dye solution at ambient temperature (25 ± 5 °C). 5 mL of sample solution was taken periodically and centrifuged to separate the catalyst. The decolourization percentage was monitored by measuring the absorbance of the supernatant at 610 nm and calculated according to the following equation:

$$\text{color removal}\,(\%) = \frac{Abs(0) - Abs(t)}{Abs(0)} \times 100 \quad (1)$$

where $Abs_{(0)}$ and $Abs_{(t)}$ are the initial absorbance and the absorbance at any time t, respectively.

2.6. Adsorption experiments

The adsorption experiments were performed in a 500 mL open Pyrex cell in the dark at natural pH (5.8) at different dye concentrations (5, 10 and 15 mg L^{-1}) with B-oPhen (solid/solution ratio: 1 g L^{-1}).

2.7. Photo-decolourization

Kinetic studies were undertaken in the absence and presence of support catalyst B-oPhen with initial dye concentration ranging from 5 to 20 mg L^{-1} and under UV-B and solar irradiation.

2.8. Reusability

The reusability experiments of B-oPhen in the photo-decolourization of indigo carmine were performed at pH 5.8 under solar irradiation with a solid/solution ratio of 1 g L^{-1} and 10 mg L^{-1} dye solution. Subsequently to total decolourization, achieved by exposing the mixture to sunlight for 160 min, the catalyst was separated by centrifugation and immediately added to a fresh 10 mg L^{-1} solution of dye in similar conditions as above. The process was repeated three times.

3. Results and discussion

3.1. Characterization of materials

The X-ray diffractogram of the exchanged bentonite B-oPhen shows a d_{001} line at 17.83 Å whereas that of sodic bentonite (B-Na) is at 14.55 Å (Fig. 3). This indicates an intercalation of the orthophenanthrolinium species in the interlayer space of the clay.

The introduction of orthophenanthrolinium species in the interlayer space of the bentonite is evidenced by IR spectroscopy analysis as shown in IR spectra (Fig. 4). The infrared characteristics of B-Na are similar to those reported for the same bentonite [41].

The 1,10-phenanthroline hydrochloride characteristic absorption bands are present in the B-oPhen sample spectrum particularly those observed in the wavenumber range from 1420 to 1540 cm^{-1}.

This observation is confirmed by the MAS ^{13}C spectrum of B-oPhen in which the three peaks at 127, 136 and 140 ppm are shown in Fig. 5. These chemical shift values are characteristics of orthophenanthroline aromatic ring carbons.

The thermogravimetric plots of B-Na and B-oPhen are shown in Fig. 6. The thermogravimetric plot of B-oPhen shows a 2% initial

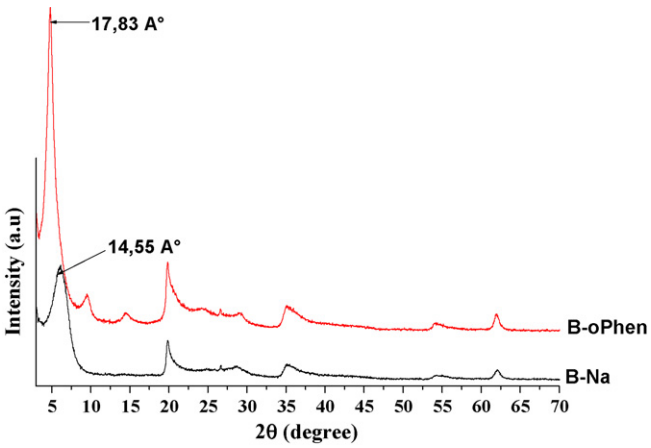

Fig. 3. PXRD spectra of B-Na and B-oPhen.

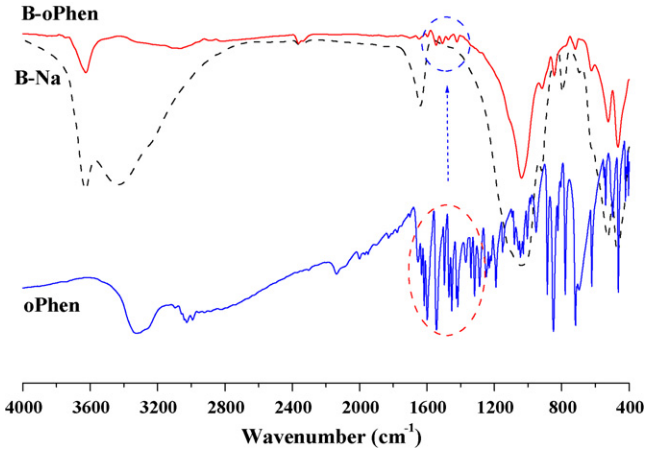

Fig. 4. FT-IR spectra of B-Na, B-oPhen and oPhen.

weight loss (25–150 °C) due to the interlayer and coordinated water and 10.35% (330–550 °C) which could be attributed to the interlayer orthophenanthrolinium decomposition. This 10.35% weight loss (103.5 mg of organic compound per gram of bentonite) is greater than the exchanged amount (0.185 mmol/g or 43.4 mg/g of bentonite). The difference (103.5–43.4 = 60.1 mg/g) could be the orthophenanthroline amount bound to the iron present in the clay (B-oPhen was light red coloured).

The later observation is confirmed by the diffuse reflectance spectra of B-Na and B-oPhen materials shown in Fig. 7. The B-Na sample shows a large absorption band in the UV region with a maximum at 254 nm whereas the B-oPhen sample shows two large absorption bands in the UV and visible regions (λ_{max} at 260

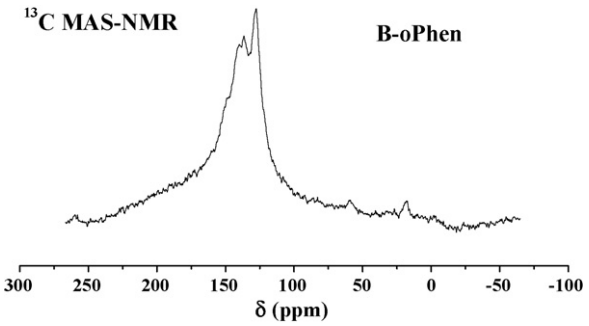

Fig. 5. ^{13}C MAS NMR spectrum of B-oPhen.

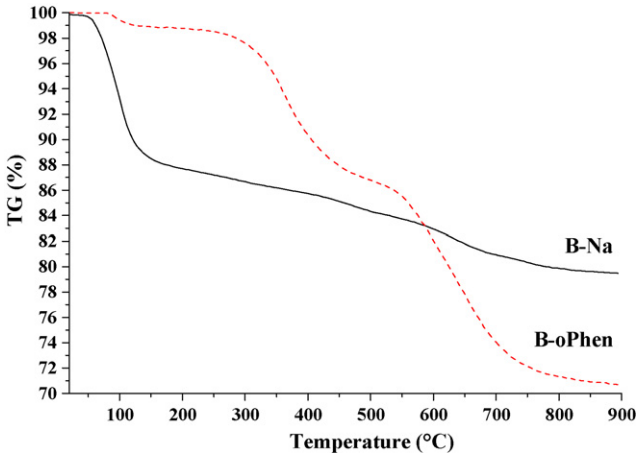

Fig. 6. TGA plots of B-Na and B-oPhen.

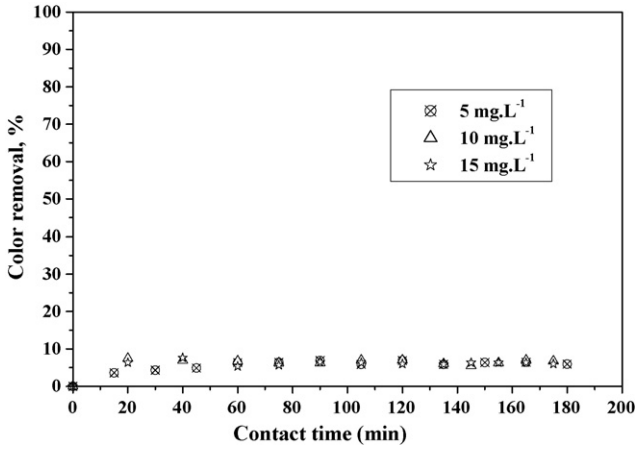

Fig. 8. Adsorption kinetic of indigo carmine on of B-oPhen ($pH_i = 5.8$ and solid/solution ratio: 1 g L^{-1}) in the dark at different dye concentrations.

and 520 nm, respectively), which may results in a photocatalytic activity improvement of B-oPhen under visible irradiation.

3.2. Adsorption kinetics in the dark

The decolourization efficiency of IC dye on B-oPhen in the absence of irradiation at different dye concentrations is shown in Fig. 8. The equilibrium time of IC dye adsorption on B-oPhen was found to be 30 min. The maximum IC dye decolourization by adsorption was about 7%. This value is very low because of the negatives charges of the dye sulfonate groups.

3.3. Photocatalytic decolourization of indigo carmine

3.3.1. Effect of the presence of B-oPhen, B-Na and of the irradiation nature on the decolourization rate

The effect of irradiation nature in the absence of B-oPhen and B-Na at 10 mg L^{-1} initial concentration of IC dye is shown in Fig. 9. The better decolourization efficiency was obtained under solar rather than UV-B irradiation, so about 10 and 5% of % decolourization were found under, respectively solar and UV-B irradiation. The indigo carmine was found to be resistant for decolourization under UV-B and solar irradiation in the absence of B-oPhen. The presence of B-Na has no effect on the decolourization of IC under UV-B and solar irradiation.

The presence of B-oPhen increases considerably the % decolourization. Fig. 9 shows that under solar irradiation a practically total colour removal was obtained after 160 min of contact time. However, under UV-B irradiation the decolourization rate is slower.

3.3.2. Kinetic modelling

According to several works [42,43], the kinetic of the photocatalytic decolourization rate of most organic compounds is described by the pseudo-first order kinetic model.

$$-\frac{dC}{dt} = k_{app}C \quad (2)$$

where k_{app} (min^{-1}) is the apparent rate constant.

Integration of Eq. (2) leads to the following relation (with the respect of the limit condition: $C_t = C_0$ at $t = 0$).

$$\ln\left(\frac{C_0}{C_t}\right) = k_{app}t \quad (3)$$

At low concentration of dye (diluted solution) and using the dye concentration–absorbance relationship ($Abs = C\varepsilon l$) Eq. (3) can be rewritten as:

$$\ln\left(\frac{Abs_0}{Abs_t}\right) = k_{app}t \quad (4)$$

k_{app} values for each initial concentration and under UV-B and solar irradiation were found from the slopes of straight line obtained by plotting $\ln(Abs_0/Abs_t)$ versus reaction time. Fig. 10 shows that the photocatalytic decolourization kinetic data fit the pseudo-first order kinetic with good values of the determination

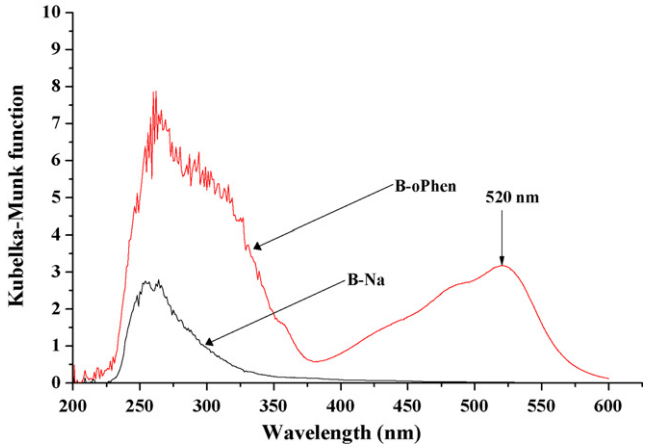

Fig. 7. The UV–vis diffuse reflectance spectra of B-Na and B-oPhen.

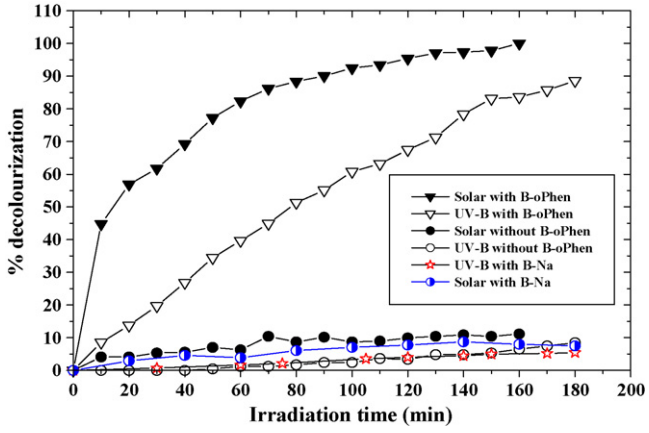

Fig. 9. Kinetics of indigo carmine photo-decolourization ($C_i = 10$ mg L^{-1} and $pH_i = 5.8$) under solar and UV irradiations with and without materials.

Table 2
Effect of initial dye concentration and irradiation nature on photo-decolourization of indigo carmine (experimental condition: B-ophen dose 1 g L^{-1} and initial pH 5.8).

Irradiation type	[dye] (mg L^{-1})	k_{app} (min^{-1})	$t_{1/2}$ (min)	r_0 (mg L^{-1} min^{-1})	R^2
UV-B	5	0.01151	60.2	0.05755	0.9837
	10	0.00899	77.1	0.0899	0.9956
	12.5	0.00894	77.5	0.1118	0.9914
	15	0.00824	84.1	0.1236	0.9774
	20	0.00748	92.7	0.1496	0.9855
Solar	5	0.0304	22.8	0.1518	0.9908
	10	0.0263	26.4	0.2633	0.9919
	15	0.0234	29.6	0.3516	0.9945

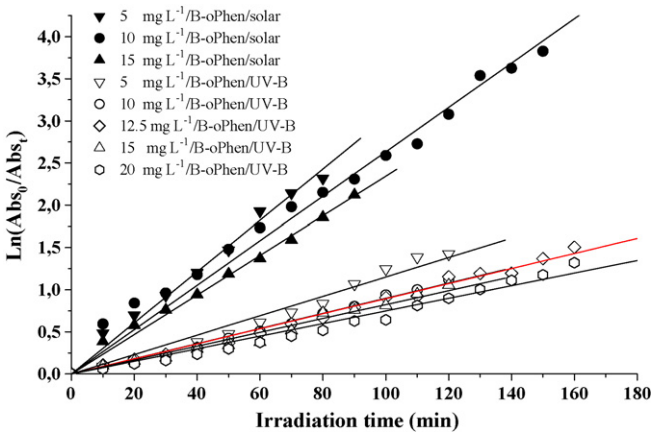

Fig. 10. Pseudo-first kinetics plot of indigo carmine photo-decolourization with B-oPhen, under solar and UV irradiations (pH_i = 5.8 and solid/solution ratio: 1 g L^{-1}).

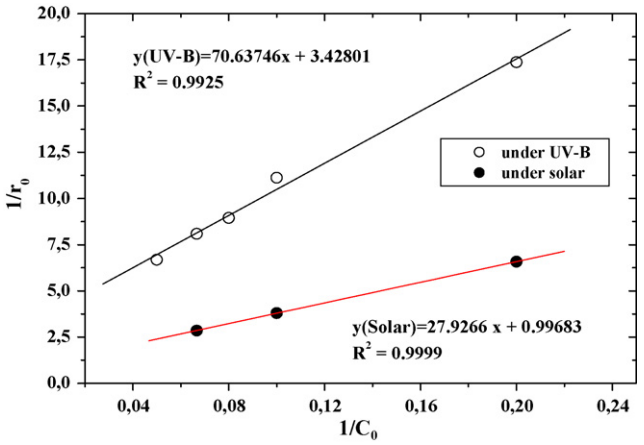

Fig. 11. Langmuir–Hinshelwood plots of indigo carmine photo-decolourization with B-oPhen, under solar and UV irradiations (pH_i = 5.8 and solid/solution ratio: 1 g L^{-1}).

coefficient ($R^2 > 0.977$) in the range of initial concentration of dye from 5 to 20 mg L^{-1}.

The values of k_{app}, half-lives ($t_{1/2}$) and initial decolourization rates at various initial concentrations of indigo carmine are given in Table 2. The highest decolourization rate and the shortest half-life of indigo carmine decolourization were observed at low dye concentration and under solar irradiation. This could be due to the contribution of the visible wavelength range of the solar spectrum since the B-oPhen material is light red colored.

Hence, the photocatalytic oxidation process is more suitable for low dye concentrations. This observation follows several reported studies [42–45].

In order to determine the relationship between the initial degradation rate and the initial concentration of the organic compounds, the Langmuir–Hinshelwood rate expression has been successfully used for heterogeneous photocatalytic degradation [42–45]:

$$r_0 = k_{app}C_0 = \frac{k_{L-H}K_{ads}C_0}{1 + K_{ads}C_0} \quad (5)$$

The linearization of Eq. (5) gives the following equation (Eq. (6)), which indicates the relationship between $1/r_0$ and $1/C_0$.

$$\frac{1}{r_0} = \frac{1}{k_{L-H}} + \frac{1}{k_{L-H}K_{ads}}\frac{1}{C_0} \quad (6)$$

where r_0 (mg L^{-1} min^{-1}) is the initial rate of the photocatalytic decolourization, k_{L-H} (mg L^{-1} min^{-1}) is the Langmuir–Hinshelwood rate constant (dependent on the nature of light irradiation and of the radiation field inside a photocatalytic reactor), K_{ads} is the adsorption equilibrium constant on B-oPhen in L mg^{-1}, and C_0 is the initial concentration of the solute (mg L).

The applicability of L–H equation for the decolourization has been confirmed by the linear plot obtained by plotting reciprocal of initial rate ($1/r_0$) against reciprocal of initial concentration ($1/C_0$) as shown in Fig. 10. The values of the rate constant k_{L-H} and of the adsorption equilibrium constant K_{ads} obtained from the intercepts and the slopes of Fig. 11 are reported in Table 3. The k_{L-H} values were 0.292 mg L^{-1} min^{-1} under UV-B irradiation and 1.003 mg L^{-1} min^{-1} under solar irradiation. This indicates a better initial decolourization rate under solar irradiation than under UV-B one.

Table 3
Langmuir–Hinshelwood parameters of indigo carmine photo-decolourization under UV-B and solar irradiation (experimental condition: B-ophen dose 1 g L^{-1} and initial pH 5.8).

Irradiation type	k_{L-H} (mg L^{-1} min^{-1})	K_{ads} (L mg^{-1})	R^2
UV-B	0.292	0.0485	0.9925
Solar	1.003	0.0357	0.9999

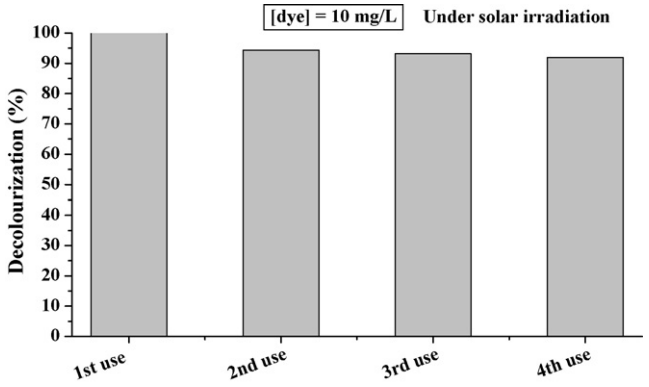

Fig. 12. % Colour removal after reuse of B-oPhen (C_i = 10 mg L^{-1}, pH_i = 5.8 and solid/solution ratio: 1 g L^{-1}).

3.3.3. Photocatalyst reuse study

The reuse of photocatalyst for photo-decolourization of 10 mg L^{-1} of indigo carmine solution is presented in Fig. 12. No more less than 90% of photo-decolourization of indigo carmine was observed after three times of photocatalyst reuse. The photocatalyst B-oPhen present a good stability for photocatalytic decolourization after 4 uses.

4. Conclusion

In the present work, organophilic clay was prepared and characterized by XRD, FT-IR, TGA and ^{13}C MAS NMR. The obtained material was investigated for the photocatalytic decolourization of indigo carmine under UV-B and solar irradiation. The kinetic data were found in a good accordance with pseudo-first order and Langmuir–Hinshelwood kinetic models. The photodecolourization rate was found better under solar irradiation.

The prepared material had been subjected to three reuses with a slight loss of efficiency after the first use and the same % decolourization during the three reuses. Investigations are in progress in order to elucidate the decolourization mechanism.

Acknowledgements

The author thanks Bruno Alonso from Team Materials for catalysis and Health (MACS) of the Institute Charles Gerhardt - UMR 5253 (CNRS/ENSCM/UM2/UM1) Montpellier (France) for his help in the characterization DRS UV–vis.

References

[1] D.L. Jeffords, P.H. Lance, W.C. Dewolf, Urology 9 (1977) 180–181.
[2] I. Othman, R.M. Mohamed, I.A. Ibrahim, M.M. Mohamed, Appl. Catal. A 299 (2006) 95–102.
[3] K. Ikeda, Y. Sannohe, S. Araki, S. Inutsuka, Endoscopy 14 (1982) 119–123.
[4] W.F. Kennedy, K. Wirjoatmadja, T.J. Akamatsu, J.J. Bonica, J. Urol. 100 (1968) 775–778.
[5] J.F. Porter, G. McKay, K.H. Choy, Chem. Eng. Sci. 54 (1999) 5863–5885.
[6] V. Golob, A. Ojstresk, Dyes Pigm. 64 (2005) 57–61.
[7] P.C. Vandervivere, R. Bianchi, W. Verstraete, J. Chem. Technol. Biotechnol. 72 (1998) 289–302.
[8] R. Sanghi, B. Bhattacharya, Water Qual. Res. J. Can. 38 (2003) 553–562.
[9] W.T. Tsai, Y.M. Chang, C.W. Lai, C.C. Lo, Appl. Clay Sci. 29 (2005) 149–154.
[10] A. Tor, Y. Cengeloglu, J. Hazard. Mater. 138 (2006) 409–415.
[11] M.X. Zhu, Y.P. Li, M. Xie, H.Z. Xin, J. Hazard. Mater. 120 (2005) 163–171.
[12] V. Calabro, G. Pantano, R. Kang, R. Molinari, E. Drioli, Desalination 78 (1990) 257–277.
[13] S. Nam, P.G. Tratnyek, Water Res. 34 (2000) 1837–1845.
[14] F. Zhang, A. Yediler, X. Liang, A. Kettrup, Dyes Pigm. 60 (2004) 1–7.
[15] M. Muthukumar, D. Sargunamani, M. Senthilkumar, N. Selvakumar, Dyes Pigm. 64 (2005) 39–44.
[16] B. Wawrzyniak, A.W. Morawski, Appl. Catal. B 62 (2006) 150–158.
[17] H.Y. Shu, M.C. Chang, Dyes Pigm. 65 (2005) 25–31.
[18] S. Senthilkumaar, K. Porkodi, R. Vidyalakshmi, J. Photochem. Photobiol. A 170 (2005) 225–232.
[19] T. Velegraki, I. Poulios, M. Charalabaki, N. Kalogerakis, P. Samaras, D. Mantzavinos, Appl. Catal. B 62 (2006) 159–168.
[20] M.A. Hasnat, I.A. Siddiquey, A. Nuruddin, Dyes Pigm. 66 (2005) 185–188.
[21] R. Andreozzi, V. Caprio, A. Insola, R. Marotta, Catal. Today 53 (1999) 51–59.
[22] A.B. Prevot, C. Baiocchi, M.C. Brussino, E. Pramauro, P. Savarino, V. Augugliaro, et al., Environ. Sci. Technol. 35 (2001) 971–976.
[23] K. Vinodgopal, P.V. Kamat, J. Photochem. Photobiol. A 83 (1994) 141–146.
[24] Y. Xu, C.H. Langford, Langmuir 17 (2001) 897–902.
[25] M. Saquib, M. Muneer, Dyes Pigm. 53 (2002) 237–249.
[26] M. Muneer, R. Philips, S. Das, Res. Chem. Intermed. 23 (1997) 233–246.
[27] C. Hachem, F. Bocquillon, O. Zahraa, M. Bouchy, Dyes Pigm. 49 (2001) 117–125.
[28] V. Ramaswamy, M. Sivarama Krishnan, A.V. Ramaswamy, J. Mol. Catal. A 181 (2002) 81–89.
[29] M. Yagi, K. Narita, J. Am. Chem. Soc. 126 (2004) 8084–8085.
[30] M.A. Vicente, C. Belver, R. Trujillano, V. Rives, A.C. Alvarez, J.-F. Lambert, S.A. Korili, L.M. Gandıĭa, A. Gil, Appl. Catal. A: Gen. 267 (2004) 47–58.
[31] J. Pires, J. Francisco, A. Carvalho, M.B. de Carvalho, A.R. Silva, C. Freire, B. de Castro, Langmuir 20 (2004) 2861–2866.
[32] A.M. Machado, F. Wypych, S.M. Drechsel, S. Nakagaki, J. Colloid Interface Sci. 254 (2002) 158–164.
[33] T.J. Pinnavaia, Intercalated clay catalyst, Science 220 (1983) 365–371.
[34] N. Sanabria, A. Alvarez, R. Molina, S. Moreno, Catal. Today 133–135 (2008) 530–533.
[35] M. Cheng, W. Song, W. Ma, C. Cheng, J. Zhao, J. Lin, H. Zhu, Appl. Catal. B 77 (2008) 355–363.
[36] J. Feng, X. Hu, P.L. Yue, Water Res. 39 (2005) 89–96.
[37] M. Cheng, W. Ma, C. Chen, J. Yao, J. Zhao, Appl. Catal. B 65 (2006) 217–226.
[38] A. Bentouami, M.S. Ouali, J. Colloid Interface Sci. 293 (2006) 270–277.
[39] C. Abdelouahab, H. Ait Amar, T.Z. Obretenov, A. Gaid, Analysis 16 (1988) 292–299.
[40] G. Kahr, F.T. Madsen, Appl. Clay Sci. 9 (1995) 327–336.
[41] A. Bakhti, Z. Derriche, A. Iddou, M. Larid, Eur. J. Soil Sci. 52 (2001) 683–692.
[42] A.P. Toor, A. Verma, C.K. Jotshi, P.K. Bajpai, V. Singh, Dyes Pigm. 68 (2006) 53–60.
[43] S. Senthilkumaar, K. Porkodi, J. Colloid Interface Sci. 288 (2005) 184–189.
[44] M. Muruganandham, M. Swaminathan, Dyes Pigm. 68 (2006) 133–142.
[45] E. Evgenidou, K. Fytianos, I. Poulios, Catal. Appl. B 59 (2005) 83–91.